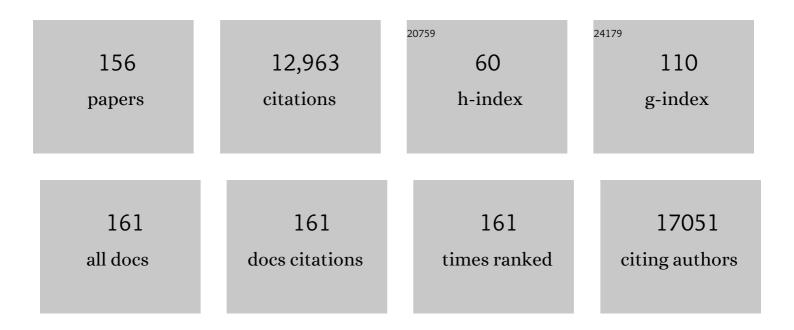
Yang Yang

List of Publications by Year in descending order

Source: https://exaly.com/author-pdf/4507316/publications.pdf Version: 2024-02-01



VANC VANC

#	Article	IF	CITATIONS
1	A multi-step induced strategy to fabricate core-shell Pt-Ni alloy as symmetric electrocatalysts for overall water splitting. Nano Research, 2022, 15, 965-971.	5.8	41
2	Perovskite solar cells based self-charging power packs: Fundamentals, applications and challenges. Nano Energy, 2022, 94, 106910.	8.2	41
3	Atomically dispersed catalysts for small molecule electrooxidation in direct liquid fuel cells. Journal of Energy Chemistry, 2022, 68, 439-453.	7.1	18
4	Manipulating the Electronic Structure of Graphite Intercalation Compounds for Boosting the Bifunctional Oxygen Catalytic Performance. Small, 2022, 18, e2107667.	5.2	11
5	Surface oxygenation induced strong interaction between Pd catalyst and functional support for zinc–air batteries. Energy and Environmental Science, 2022, 15, 1573-1584.	15.6	49
6	Iron Catalyzed Cascade Construction of Molybdenum Carbide Heterointerfaces for Understanding Hydrogen Evolution. Small, 2022, 18, e2200439.	5.2	8
7	Achieving ultra-long lifespan Zn metal anodes by manipulating desolvation effect and Zn deposition orientation in a multiple cross-linked hydrogel electrolyte. Energy Storage Materials, 2022, 49, 172-180.	9.5	77
8	Organophosphine ligand derived sandwich-structural electrocatalyst for oxygen evolution reaction. Journal of Energy Chemistry, 2022, 70, 74-83.	7.1	9
9	Activating the Stepwise Intercalation–Conversion Reaction of Layered Copper Sulfide toward Extremely High Capacity Zinc-Metal-Free Anodes for Rocking-Chair Zinc-Ion Batteries. ACS Applied Materials & Interfaces, 2022, 14, 1126-1137.	4.0	26
10	Porous FeCo Glassy Alloy as Bifunctional Support for Highâ€Performance Znâ€Air Battery. Advanced Energy Materials, 2021, 11, 2002204.	10.2	55
11	Polymer-Derived Ceramic Nanoparticle/Edge-Functionalized Graphene Oxide Composites for Lithium-Ion Storage. ACS Applied Materials & Interfaces, 2021, 13, 9794-9803.	4.0	9
12	Rational Assembly of Superstructure Microparticles into Mosaic‣ike Highly Oriented Monolayer for Glucoseâ€Responsive Electrodes. Advanced Materials Interfaces, 2021, 8, 2100433.	1.9	0
13	Ultimate Resourcization of Waste: Crab Shell-Derived Biochar for Antimony Removal and Sequential Utilization as an Anode for a Li-Ion Battery. ACS Sustainable Chemistry and Engineering, 2021, 9, 8813-8823.	3.2	28
14	Dualâ€Doping and Synergism toward Highâ€Performance Seawater Electrolysis. Advanced Materials, 2021, 33, e2101425.	11.1	161
15	CO ₂ Bubble-Assisted Pt Exposure in PtFeNi Porous Film for High-Performance Zinc-Air Battery. Journal of the American Chemical Society, 2021, 143, 11595-11601.	6.6	34
16	Recent Advances in Electrode Design for Rechargeable Zinc–Air Batteries. Small Science, 2021, 1, 2100044.	5.8	47
17	Insights into adsorptive removal of antimony contaminants: Functional materials, evaluation and prospective. Journal of Hazardous Materials, 2021, 418, 126345.	6.5	47
18	Layer Orientation-Engineered Two-Dimensional Platinum Ditelluride for High-Performance Direct Alcohol Fuel Cells. ACS Energy Letters, 2021, 6, 3481-3487.	8.8	12

#	Article	IF	CITATIONS
19	Doping-modulated strain control of bifunctional electrocatalysis for rechargeable zinc–air batteries. Energy and Environmental Science, 2021, 14, 5035-5043.	15.6	39
20	Stable, high-performance, dendrite-free, seawater-based aqueous batteries. Nature Communications, 2021, 12, 237.	5.8	174
21	Enhanced activity towards oxygen electrocatalysis for rechargeable Zn–air batteries by alloying Fe and Co in N-doped carbon. Dalton Transactions, 2021, 50, 16185-16190.	1.6	6
22	Rational Synthesis of Polymeric Nitrogen N ₈ [–] with Ultraviolet Irradiation and Its Oxygen Reduction Reaction Mechanism Study with In Situ Shell-Isolated Nanoparticle-Enhanced Raman Spectroscopy. ACS Catalysis, 2021, 11, 13034-13040.	5.5	3
23	Improving Pd–N–C fuel cell electrocatalysts through fluorination-driven rearrangements of local coordination environment. Nature Energy, 2021, 6, 1144-1153.	19.8	108
24	A mini-review: emerging all-solid-state energy storage electrode materials for flexible devices. Nanoscale, 2020, 12, 3560-3573.	2.8	73
25	Promoting nitrogen photofixation over a periodic WS ₂ @TiO ₂ nanoporous film. Journal of Materials Chemistry A, 2020, 8, 1059-1065.	5.2	44
26	Nickelâ€Catalyzed Synthesis of 3D Edgeâ€Curled Graphene for Highâ€Performance Lithiumâ€Ion Batteries. Advanced Functional Materials, 2020, 30, 1904645.	7.8	32
27	Optimization of Catalytic Sites in Cobaltâ€Modified Nitrogenâ€Doped Carbon towards Highâ€Performance Oxygen Reduction Electrocatalysts for Zincâ€Air Batteries. ChemElectroChem, 2020, 7, 421-427.	1.7	11
28	Stable Fe ₂ P ₂ S ₆ Nanocrystal Catalyst for High‣fficiency Water Electrolysis. Small Methods, 2020, 4, 1900632.	4.6	29
29	Stabilizing atomic Pt with trapped interstitial F in alloyed PtCo nanosheets for high-performance zinc-air batteries. Energy and Environmental Science, 2020, 13, 884-895.	15.6	99
30	Boosting alkaline hydrogen evolution: the dominating role of interior modification in surface electrocatalysis. Energy and Environmental Science, 2020, 13, 3110-3118.	15.6	87
31	Stabilizing Atomically Dispersed Catalytic Sites on Tellurium Nanosheets with Strong Metal–Support Interaction Boosts Photocatalysis. Small, 2020, 16, e2002356.	5.2	45
32	Carbon foams: 3D porous carbon materials holding immense potential. Journal of Materials Chemistry A, 2020, 8, 23699-23723.	5.2	86
33	Stabilization of Sn Anode through Structural Reconstruction of a Cu–Sn Intermetallic Coating Layer. Advanced Materials, 2020, 32, e2003684.	11.1	53
34	Designing CO ₂ reduction electrode materials by morphology and interface engineering. Energy and Environmental Science, 2020, 13, 2275-2309.	15.6	251
35	Significantly Improved Cyclability of Conversionâ€₹ype Transition Metal Oxyfluoride Cathodes by Homologous Passivation Layer Reconstruction. Advanced Energy Materials, 2020, 10, 1903333.	10.2	33
36	Functionally Graded Materials for Long-Cycle Lithium-Ion Batteries. ECS Meeting Abstracts, 2020, MA2020-01, 151-151.	0.0	0

#	Article	IF	CITATIONS
37	Atomic Pt with Trapped Interstitial F in PtCo Nanosheets for Zinc-Air Batteries. ECS Meeting Abstracts, 2020, MA2020-01, 2793-2793.	0.0	0
38	Programmable Electrodeposition of Ptni Alloy Porous Film for Oxygen Reduction. ECS Meeting Abstracts, 2020, MA2020-01, 1162-1162.	0.0	0
39	(Invited) Promoted Nitrogen Photofixation over Periodic WS2@TiO2 Nanoporous Film. ECS Meeting Abstracts, 2020, MA2020-01, 1732-1732.	0.0	0
40	(Invited) Plasmon-Enhanced Sensors Using Heterogeneous Films. ECS Meeting Abstracts, 2020, MA2020-01, 1422-1422.	0.0	0
41	Programmable Exposure of Pt Active Facets for Efficient Oxygen Reduction. Angewandte Chemie, 2019, 131, 15995-16001.	1.6	14
42	Programmable Exposure of Pt Active Facets for Efficient Oxygen Reduction. Angewandte Chemie - International Edition, 2019, 58, 15848-15854.	7.2	81
43	Partially sulfurated ultrathin nickel-iron carbonate hydroxides nanosheet boosting the oxygen evolution reaction. Electrochimica Acta, 2019, 309, 57-64.	2.6	37
44	S-Doped MoP Nanoporous Layer Toward High-Efficiency Hydrogen Evolution in pH-Universal Electrolyte. ACS Catalysis, 2019, 9, 651-659.	5.5	167
45	Self‣upported Tin Sulfide Porous Films for Flexible Aluminumâ€ŀon Batteries. Advanced Energy Materials, 2019, 9, 1802543.	10.2	110
46	(003)-Facet-exposed Ni3S2 nanoporous thin films on nickel foil for efficient water splitting. Applied Catalysis B: Environmental, 2019, 243, 693-702.	10.8	129
47	Phase and Defect Engineering of MoS ₂ Stabilized in Periodic TiO ₂ Nanoporous Film for Enhanced Solar Water Splitting. Advanced Optical Materials, 2019, 7, 1801403.	3.6	25
48	Apically Dominant Mechanism for Improving Catalytic Activities of Nâ€Đoped Carbon Nanotube Arrays in Rechargeable Zinc–Air Battery. Advanced Energy Materials, 2018, 8, 1800480.	10.2	153
49	Enhancing Electron Transfer and Electrocatalytic Activity on Crystalline Carbon-Conjugated g-C ₃ N ₄ . ACS Catalysis, 2018, 8, 1926-1931.	5.5	172
50	Photocatalytic glycerol oxidation on Au _x Cu–CuS@TiO ₂ plasmonic heterostructures. Journal of Materials Chemistry A, 2018, 6, 22005-22012.	5.2	41
51	Phosphorus and Aluminum Codoped Porous NiO Nanosheets as Highly Efficient Electrocatalysts for Overall Water Splitting. ACS Energy Letters, 2018, 3, 892-898.	8.8	130
52	Integration of Au nanoparticles with a g-C ₃ N ₄ based heterostructure: switching charge transfer from type-II to Z-scheme for enhanced visible light photocatalysis. Chemical Communications, 2018, 54, 3747-3750.	2.2	56
53	Structure, electrical and dielectric properties of Ca substituted BaTiO3 ceramics. Ceramics International, 2018, 44, 11109-11115.	2.3	59
54	MoS ₂ /TiO ₂ heterostructures as nonmetal plasmonic photocatalysts for highly efficient hydrogen evolution. Energy and Environmental Science, 2018, 11, 106-114.	15.6	326

#	Article	IF	CITATIONS
55	Surfaceâ€Modified Porous Carbon Nitride Composites as Highly Efficient Electrocatalyst for Znâ€Air Batteries. Advanced Energy Materials, 2018, 8, 1701642.	10.2	129
56	Freestanding NiFe Oxyfluoride Holey Film with Ultrahigh Volumetric Capacitance for Flexible Asymmetric Supercapacitors. Small, 2018, 14, 1702295.	5.2	34
57	Use of a diatomite template to prepare a MoS ₂ /amorphous carbon composite and exploration of its electrochemical properties as a supercapacitor. RSC Advances, 2018, 8, 35672-35680.	1.7	11
58	Understanding Synergism of Cobalt Metal and Copper Oxide toward Highly Efficient Electrocatalytic Oxygen Evolution. ACS Catalysis, 2018, 8, 12030-12040.	5.5	60
59	Room-Temperature-and-Pressure Vapor Deposition of Trace Amount of Pyrrole for Improving the Ageing Resistance and Electrochemical Performance of LiFePO ₄ /C. Journal of the Electrochemical Society, 2018, 165, A3136-A3143.	1.3	6
60	Graphitic Carbon Nitride for Electrochemical Energy Conversion and Storage. ACS Energy Letters, 2018, 3, 2796-2815.	8.8	149
61	Amorphous MOF Introduced N-Doped Graphene: An Efficient and Versatile Electrocatalyst for Zinc–Air Battery and Water Splitting. ACS Applied Energy Materials, 2018, 1, 2440-2445.	2.5	64
62	Drastic enhancement of photoelectrochemical water splitting performance over plasmonic Al@TiO2 heterostructured nanocavity arrays. Nano Energy, 2018, 51, 400-407.	8.2	64
63	A synergistic interaction between isolated Au nanoparticles and oxygen vacancies in an amorphous black TiO ₂ nanoporous film: toward enhanced photoelectrochemical water splitting. Journal of Materials Chemistry A, 2018, 6, 12978-12984.	5.2	44
64	Cobalt nanocrystals embedded into N-doped carbon as highly active bifunctional electrocatalysts from pyrolysis of triazolebenzoate complex. Electrochimica Acta, 2018, 284, 733-741.	2.6	13
65	Nickel Sulfide Freestanding Holey Films as Air-Breathing Electrodes for Flexible Zn–Air Batteries. Journal of Physical Chemistry Letters, 2018, 9, 2746-2750.	2.1	19
66	Interface-engineered hematite nanocones as binder-free electrodes for high-performance lithium-ion batteries. Journal of Materials Chemistry A, 2018, 6, 13968-13974.	5.2	18
67	N, Pâ€doped CoS ₂ Embedded in TiO ₂ Nanoporous Films for Zn–Air Batteries. Advanced Functional Materials, 2018, 28, 1804540.	7.8	93
68	Periodically Ordered Nanoporous Perovskite Photoelectrode for Efficient Photoelectrochemical Water Splitting. ACS Nano, 2018, 12, 6335-6342.	7.3	74
69	Electrochemical Fabrication of Freestanding Thin-Film Electrodes for Batteries and Catalysis. ECS Meeting Abstracts, 2018, , .	0.0	0
70	(Invited) Versatile Plasmonic Films for Sensing and Photocatalytic Applications. ECS Meeting Abstracts, 2018, , .	0.0	0
71	Electrochemical Fabrication of Nanostructured Thin-Film for Renewable Energy Applications. ECS Meeting Abstracts, 2018, , .	0.0	0
72	Electrochemical Fabrication of Nanostructured Thin-Film for Renewable Energy Applications. ECS Meeting Abstracts, 2018, , .	0.0	0

#	Article	IF	CITATIONS
73	Rational Design of Periodically Ordered Nanoporous Thin-Film Catalysts for Plasmonic Photocatalysis. ECS Meeting Abstracts, 2018, , .	0.0	0
74	Plasmonic Heterosturcture for Full Solar Spectrum Harvesting. ECS Meeting Abstracts, 2018, MA2018-01, 1873-1873.	0.0	0
75	Inorganic Porous Films for Renewable Energy Storage. ACS Energy Letters, 2017, 2, 373-390.	8.8	68
76	Green photoluminescence in Tb3+-doped ZrO2 nanotube arrays. Journal of Materials Science: Materials in Electronics, 2017, 28, 7253-7258.	1.1	9
77	Polyaniline supercapacitors. Journal of Power Sources, 2017, 347, 86-107.	4.0	723
78	Strained W(Se _{<i>x</i>} S _{1–<i>x</i>}) ₂ Nanoporous Films for Highly Efficient Hydrogen Evolution. ACS Energy Letters, 2017, 2, 1315-1320.	8.8	64
79	Ruthenium-cobalt nanoalloys encapsulated in nitrogen-doped graphene as active electrocatalysts for producing hydrogen in alkaline media. Nature Communications, 2017, 8, 14969.	5.8	656
80	Tuning Electronic Structures of Nonprecious Ternary Alloys Encapsulated in Graphene Layers for Optimizing Overall Water Splitting Activity. ACS Catalysis, 2017, 7, 469-479.	5.5	342
81	Periodically Patterned Au-TiO ₂ Heterostructures for Photoelectrochemical Sensor. ACS Sensors, 2017, 2, 621-625.	4.0	86
82	Three-Dimensional Dendritic Structures of NiCoMo as Efficient Electrocatalysts for the Hydrogen Evolution Reaction. ACS Applied Materials & amp; Interfaces, 2017, 9, 22420-22431.	4.0	100
83	A freestanding NiS _x porous film as a binder-free electrode for Mg-ion batteries. Chemical Communications, 2017, 53, 7608-7611.	2.2	54
84	Overall Water Splitting with Room-Temperature Synthesized NiFe Oxyfluoride Nanoporous Films. ACS Catalysis, 2017, 7, 8406-8412.	5.5	91
85	Environment-benign synthesis of rGO/MnO nanocomposites with superior electrochemical performance for supercapacitors. Journal of Alloys and Compounds, 2017, 729, 9-18.	2.8	32
86	Synergistically assembled MWCNT/graphene foam with highly efficient microwave absorption in both C and X bands. Carbon, 2017, 124, 506-514.	5.4	297
87	One-dimensional hematite photoanodes with spatially separated Pt and FeOOH nanolayers for efficient solar water splitting. Journal of Materials Chemistry A, 2017, 5, 17056-17063.	5.2	55
88	NiS ₂ /FeS Holey Film as Freestanding Electrode for Highâ€Performance Lithium Battery. Advanced Energy Materials, 2017, 7, 1701309.	10.2	99
89	CVD-grown polypyrrole nanofilms on highly mesoporous structure MnO2 for high performance asymmetric supercapacitors. Chemical Engineering Journal, 2017, 307, 105-112.	6.6	135
90	(Invited) A Versatile Plasmonic Film for Biosensing and Photocatalytic Applications. ECS Meeting Abstracts, 2017, , .	0.0	0

#	Article	IF	CITATIONS
91	Strengthening of Lightweight Thin-Film Electrodes with Metal-Filaments for Renewable Energy Applications. ECS Meeting Abstracts, 2017, , .	0.0	0
92	Enhanced Photoelectrocatalytic Reduction of Oxygen Using Au@TiO ₂ Plasmonic Film. ACS Applied Materials & Interfaces, 2016, 8, 34970-34977.	4.0	52
93	Straightforward synthesis of hierarchical Co3O4@CoWO4/rGO core–shell arrays on Ni as hybrid electrodes for asymmetric supercapacitors. Ceramics International, 2016, 42, 10719-10725.	2.3	64
94	Nitrogen-doped carbonized cotton for highly flexible supercapacitors. Carbon, 2016, 105, 260-267.	5.4	108
95	Flexible Nanoporous WO _{3–<i>x</i>} Nonvolatile Memory Device. ACS Nano, 2016, 10, 7598-7603.	7.3	114
96	Sandwich structured graphene-wrapped FeS-graphene nanoribbons with improved cycling stability for lithium ion batteries. Nano Research, 2016, 9, 2904-2911.	5.8	52
97	Outstanding supercapacitive properties of Mn-doped TiO2 micro/nanostructure porous film prepared by anodization method. Scientific Reports, 2016, 6, 22634.	1.6	35
98	Highâ€₽erformance Pseudocapacitive Microsupercapacitors from Laserâ€Induced Graphene. Advanced Materials, 2016, 28, 838-845.	11.1	439
99	Ultrafine V ₂ O ₅ Nanowires in 3D Current Collector for Highâ€Performance Supercapacitor. ChemElectroChem, 2016, 3, 704-708.	1.7	31
100	Ultrahigh Voltage Synthesis of 2D Amorphous Nickel-Cobalt Hydroxide Nanosheets on CFP for High Performance Energy Storage Device. Electrochimica Acta, 2016, 190, 695-702.	2.6	46
101	Vertically Aligned WS ₂ Nanosheets for Water Splitting. Advanced Functional Materials, 2015, 25, 6199-6204.	7.8	108
102	Enhanced Cycling Stability of Lithiumâ€lon Batteries Using Grapheneâ€Wrapped Fe ₃ O ₄ â€Graphene Nanoribbons as Anode Materials. Advanced Energy Materials, 2015, 5, 1500171.	10.2	133
103	Tungsten-based porous thin-films for electrocatalytic hydrogen generation. Journal of Materials Chemistry A, 2015, 3, 5798-5804.	5.2	43
104	Atomic H-induced cutting and unzipping of single-walled carbon nanotube carpets with a teepee structure and their enhanced supercapacitor performance. Journal of Materials Chemistry A, 2015, 3, 10077-10084.	5.2	14
105	Porous Cobaltâ€Based Thin Film as a Bifunctional Catalyst for Hydrogen Generation and Oxygen Generation. Advanced Materials, 2015, 27, 3175-3180.	11.1	460
106	Cobalt Nanoparticles Embedded in Nitrogen-Doped Carbon for the Hydrogen Evolution Reaction. ACS Applied Materials & Interfaces, 2015, 7, 8083-8087.	4.0	180
107	Non-precious alloy encapsulated in nitrogen-doped graphene layers derived from MOFs as an active and durable hydrogen evolution reaction catalyst. Energy and Environmental Science, 2015, 8, 3563-3571.	15.6	498
108	Three-Dimensional Networked Nanoporous Ta ₂ O _{5–<i>x</i>} Memory System for Ultrahigh Density Storage. Nano Letters, 2015, 15, 6009-6014.	4.5	50

#	Article	IF	CITATIONS
109	Carbon-Free Electrocatalyst for Oxygen Reduction and Oxygen Evolution Reactions. ACS Applied Materials & Interfaces, 2015, 7, 20607-20611.	4.0	39
110	Rebar Graphene. ACS Nano, 2014, 8, 5061-5068.	7.3	178
111	Preparation of carbon-coated iron oxide nanoparticles dispersed on graphene sheets and applications as advanced anode materials for lithium-ion batteries. Nano Research, 2014, 7, 502-510.	5.8	102
112	Three-Dimensional Nanoporous Fe ₂ O ₃ /Fe ₃ C-Graphene Heterogeneous Thin Films for Lithium-Ion Batteries. ACS Nano, 2014, 8, 3939-3946.	7.3	167
113	Direct chemical conversion of graphene to boron- and nitrogen- and carbon-containing atomic layers. Nature Communications, 2014, 5, 3193.	5.8	198
114	Edgeâ€Oriented MoS ₂ Nanoporous Films as Flexible Electrodes for Hydrogen Evolution Reactions and Supercapacitor Devices. Advanced Materials, 2014, 26, 8163-8168.	11.1	552
115	Enhanced Cycling Stability of Lithium Sulfur Batteries Using Sulfur–Polyaniline–Graphene Nanoribbon Composite Cathodes. ACS Applied Materials & Interfaces, 2014, 6, 15033-15039.	4.0	80
116	Hydrothermally Formed Three-Dimensional Nanoporous Ni(OH) ₂ Thin-Film Supercapacitors. ACS Nano, 2014, 8, 9622-9628.	7.3	148
117	Efficient Electrocatalytic Oxygen Evolution on Amorphous Nickel–Cobalt Binary Oxide Nanoporous Layers. ACS Nano, 2014, 8, 9518-9523.	7.3	359
118	Nanoporous Silicon Oxide Memory. Nano Letters, 2014, 14, 4694-4699.	4.5	62
119	LiFePO4 nanoparticles encapsulated in graphene nanoshells for high-performance lithium-ion battery cathodes. Chemical Communications, 2014, 50, 7117.	2.2	47
120	Formation of aligned nanoporous/nanotubular layers of vanadium oxy-nitrides. Electrochemistry Communications, 2014, 43, 31-35.	2.3	8
121	Graphene Nanoribbon/V ₂ O ₅ Cathodes in Lithium-Ion Batteries. ACS Applied Materials & Interfaces, 2014, 6, 9590-9594.	4.0	96
122	Three-Dimensional Thin Film for Lithium-Ion Batteries and Supercapacitors. ACS Nano, 2014, 8, 7279-7287.	7.3	50
123	Flexible Three-Dimensional Nanoporous Metal-Based Energy Devices. Journal of the American Chemical Society, 2014, 136, 6187-6190.	6.6	108
124	Nanocomposite of Polyaniline Nanorods Grown on Graphene Nanoribbons for Highly Capacitive Pseudocapacitors. ACS Applied Materials & Interfaces, 2013, 5, 6622-6627.	4.0	171
125	Evaluation of nanostructured vanadium(v) oxide in catalytic oxidations. Catalysis Science and Technology, 2013, 3, 2610.	2.1	7
126	N-Doped lepidocrocite nanotubular arrays: hydrothermal formation from anodic TiO2nanotubes and enhanced visible light photoresponse. Journal of Materials Chemistry A, 2013, 1, 1860-1866.	5.2	13

#	Article	IF	CITATIONS
127	Polypyrrole doped with redox-active poly(2-methoxyaniline-5-sulfonic acid) for lithium secondary batteries. RSC Advances, 2013, 3, 5447.	1.7	27
128	Formation of Highly Ordered Nanochannel Nb Oxide by Selfâ€Organizing Anodization. Chemistry - A European Journal, 2012, 18, 9521-9524.	1.7	35
129	Synthesis and electrochemical characterization of LiFePO4/C-polypyrrole composite prepared by a simple chemical vapor deposition method. Journal of Solid State Electrochemistry, 2012, 16, 1383-1388.	1.2	19
130	Nb-doping of TiO2/SrTiO3 nanotubular heterostructures for enhanced photocatalytic water splitting. Electrochemistry Communications, 2012, 17, 56-59.	2.3	39
131	Formation of Highly Ordered VO ₂ Nanotubular/Nanoporous Layers and Their Supercooling Effect in Phase Transitions. Advanced Materials, 2012, 24, 1571-1575.	11.1	24
132	Vertically aligned mixed V2O5–TiO2 nanotube arrays for supercapacitor applications. Chemical Communications, 2011, 47, 7746.	2.2	199
133	Electrochromic properties of anodically grown mixed V2O5–TiO2 nanotubes. Electrochemistry Communications, 2011, 13, 1021-1025.	2.3	40
134	Lithium-ion intercalation and electrochromism in ordered V2O5 nanoporous layers. Electrochemistry Communications, 2011, 13, 1198-1201.	2.3	23
135	Anodic Formation of Ti–V Binary Oxide Mesosponge Layers for Supercapacitor Applications. Chemistry - an Asian Journal, 2011, 6, 2916-2919.	1.7	8
136	Enabling the Anodic Growth of Highly Ordered V ₂ O ₅ Nanoporous/Nanotubular Structures. Angewandte Chemie - International Edition, 2011, 50, 9071-9075.	7.2	74
137	Phase transition in BaTiO3 nanotube arrays. Journal of Applied Physics, 2011, 109, 014109.	1.1	23
138	Effects of Bi ₂ O ₃ and Yb ₂ O ₃ on the Curie Temperature in BaTiO ₃ â€Based Ceramics. Journal of the American Ceramic Society, 2010, 93, 1697-1701.	1.9	23
139	CeO ₂ Nanorod–TiO ₂ Nanotube Hybrid Nanostructure. Journal of the American Ceramic Society, 2010, 93, 2555-2559.	1.9	12
140	Structure study of single crystal BaTiO ₃ nanotube arrays produced by the hydrothermal method. Nanotechnology, 2009, 20, 055709.	1.3	69
141	Superior high-rate cycling performance of LiFePO4/C-PPy composite at 55°C. Electrochemistry Communications, 2009, 11, 1277-1280.	2.3	62
142	Photoluminescence of ZnO nanorod-TiO2 nanotube hybrid arrays produced by electrodeposition. Journal of Applied Physics, 2009, 105, 094304.	1.1	29
143	Synthesis and growth mechanism of graded TiO2 nanotube arrays by two-step anodization. Materials Science and Engineering B: Solid-State Materials for Advanced Technology, 2008, 149, 58-62.	1.7	38
144	Crystallization and Phase Transition of Titanium Oxide Nanotube Arrays. Journal of the American Ceramic Society, 2008, 91, 632-635.	1.9	61

#	Article	IF	CITATIONS
145	Synthesis and Growth Mechanism of Lead Titanate Nanotube Arrays by Hydrothermal Method. Journal of the American Ceramic Society, 2008, 91, 3388-3390.	1.9	25
146	Synthesis and Photovoltaic Application of High Aspectâ€Ratio TiO ₂ Nanotube Arrays by Anodization. Journal of the American Ceramic Society, 2008, 91, 3086-3089.	1.9	25
147	Photoluminescence of Highâ€Aspectâ€Ratio PbTiO ₃ Nanotube Arrays. Journal of the American Ceramic Society, 2008, 91, 3820-3822.	1.9	20
148	Electron Field Emission and Photoluminescence of Anatase Nanotube Arrays. Journal of the American Ceramic Society, 2008, 91, 4109-4111.	1.9	20
149	Ferroelectric PbTiO3 nanotube arrays synthesized by hydrothermal method. Applied Physics Letters, 2008, 92, .	1.5	48
150	Effects of Alkalinity on the Hydrothermal Synthesis of Lead Titanate Nanotube Arrays. Journal of the American Ceramic Society, 2008, 91, 3792-3794.	1.9	5
151	Stress induced Curie temperature shift in high-aspect ratio PbTiO3 nanotube arrays. Journal of Applied Physics, 2008, 104, .	1.1	14
152	Influences of sintering atmosphere on the formation and photocatalytic property of BaFe2O4. Materials Chemistry and Physics, 2007, 105, 154-156.	2.0	33
153	Photoinduced decomposition of BaFeO3 during photodegradation of methyl orange. Journal of Molecular Catalysis A, 2007, 270, 56-60.	4.8	32
154	Photoinduced structural transformation of SrFeO3 and Ca2Fe2O5 during photodegradation of methyl orange. Materials Science and Engineering B: Solid-State Materials for Advanced Technology, 2006, 132, 311-314.	1.7	57
155	Structure and photocatalytic property of perovskite and perovskite-related compounds. Materials Chemistry and Physics, 2006, 96, 234-239.	2.0	82
156	Zinc-Doped TiO ₂ Nanotube Arrays. Key Engineering Materials, 0, 434-435, 446-447.	0.4	8